Experimental Brain Research (2024) 242:295–307
https://doi.org/10.1007/s00221-023-06746-y

RESEARCH ARTICLE

The ultrastructure of macaque mesencephalic trigeminal nucleus neurons

Niping Wang[1] · **Paul J. May**[2]

Received: 29 September 2023 / Accepted: 6 November 2023 / Published online: 1 December 2023

Abstract

Primary afferents originating from the mesencephalic trigeminal nucleus provide the main source of proprioceptive information guiding mastication, and thus represent an important component of this critical function. Unlike those of other primary afferents, their cell bodies lie within the central nervous system. It is believed that this unusual central location allows them to be regulated by synaptic input. In this study, we explored the ultrastructure of macaque mesencephalic trigeminal nucleus neurons to determine the presence and nature of this synaptic input in a primate. We first confirmed the location of macaque mesencephalic trigeminal neurons by retrograde labeling from the masticatory muscles. Since the labeled neurons were by far the largest cells located at the edge of the periaqueductal gray, we could undertake sampling for electron microscopy based on soma size. Ultrastructurally, mesencephalic trigeminal neurons had very large somata with euchromatic nuclei that sometimes displayed deeply indented nuclear membranes. Terminal profiles with varied vesicle characteristics and synaptic density thicknesses were found in contact with either their somatic plasma membranes or somatic spines. However, in contradistinction to other, much smaller, somata in the region, the plasma membranes of the mesencephalic trigeminal somata had only a few synaptic contacts. They did extend numerous somatic spines of various lengths into the neuropil, but most of these also lacked synaptic contact. The observed ultrastructural organization indicates that macaque trigeminal mesencephalic neurons do receive synaptic contacts, but despite their central location, they only avail themselves of very limited input.

Keywords Mastication · Primate · Synaptic connections · Proprioception

Introduction

The mesencephalic trigeminal nucleus (Mes V) contains the somata of primary afferent neurons, which are located sporadically along the edge of the midbrain periaqueductal gray (PAG) as individual cells and cell clusters, and also immediately lateral to the tract of Probst at the level of the locus coeruleus. Thus, the distribution of Mes V spans the mesencephalon and the rostral portion of pons. Mes V neurons have peripheral processes that innervate muscle spindles within the masticatory muscles and mechanoreceptors within periodontal ligaments (Capra et al. 1985; Byers et al. 1986; Shigenaga et al. 1988a, b, 1989; Dessem and Taylor 1989; Hassanali 1997). Among other targets, the central processes of Mes V neurons carry proprioceptive information from masticatory muscles and periodontal ligaments directly to motoneurons in the trigeminal motor nucleus, to premotor neurons in the supratrigeminal nucleus, and to the trigeminal sensory complex to provide proprioceptive information to the ascending trigeminal pathways (Luo and Li 1991; Yoshida et al. 2017).

With few exceptions (Hassanali 1997), most of the studies concerning the morphology and ultrastructure of Mes V neurons and their peripheral and central projections have been completed in non-primates (rat: Liem et al. 1991; Liem et al. 1992; Paik et al. 2005; cat: Nomura et al. 1985; Nomura and Mizuno 1985; Lazarov 1996; Honma et al. 2001). We found evidence in macaque monkeys (Wang and May 2008) that masticatory muscle afferents of Mes V have central collaterals

Communicated by Bill J Yates.

✉ Niping Wang
nwang@umc.edu

[1] Department of Periodontics and Preventive Sciences, School of Dentistry, University of Mississippi Medical Center, 2500 North State Street, Jackson, MS 39216, USA

[2] Department of Neurobiology and Anatomical Sciences, University of Mississippi Medical Center, Jackson, MS 39216, USA

that project to the trigeminal sensory complex like those of non-primates. In this previous study, we also observed axons labeled from the trigeminal sensory complex that displays close associations with Mes V somata at the light microscopic level. A number of previous studies in non-primates have indicated that Mes V cell bodies receive synaptic input from the trigeminal sensory nucleus and other sources based on the presence of close associations between labeled terminals and Mes V somata. In fact, the cerebral cortex, amygdala, habenula, reticular formation, and locus coeruleus have all been posited to project upon Mes V (rat: Minkels et al. 1991; Dessem and Luo 1999; Iida et al. 2010; Takahashi et al. 2010; Ohara et al. 2016). Similarly, transmitter-specific inputs to Mes V have been proposed based on the association of immunopositive terminal boutons with somata in the nucleus (cat: Lazarov 1995; Lazarov and Chouchkov 1996; Lazarov and Pilgrim 1997; rat: Liem et al. 1997; Bae et al. 2018). In light of these associations, it has been proposed that one of the reasons the Mes V somata have a central location, as opposed to the typical location of primary afferent somata in peripheral ganglia, is so that their activity can be modulated by these inputs. However, only in a few cases have axon terminals from specific sources been ultrastructurally demonstrated to make synaptic contacts onto Mes V somata (rat: Chen et al. 2001). Indeed, synaptic contacts on Mes V cell bodies are relatively rare according to non-primate electron microscopic studies (cat: Lazarov 1996; Honma et al. 2001; rat: Liem et al. 1991; Liem et al. 1992).

As noted above, our previous study suggests that the primate trigeminal sensory nucleus not only receives proprioceptive input, it may also send feedback to Mes V neurons. Exploration of the synaptic connections like these between Mes V and other central nuclei may tell us more about its roles in complicated masticatory activity, and how the jaw-jerk reflex and periodontal-masseteric reflex may be modulated. However, even this one connection has not been proven at the ultrastructural level in primates, and there is, to the best of our knowledge, no ultrastructural information on Mes V synaptology available in primates. Our present study investigated the ultrastructural features of retrogradely labeled and unlabeled Mes V neurons in macaque monkeys, with specific emphasis on looking for axon terminals in contact with Mes V somata. We hope that this morphological evidence will provide insight on whether and how Mes V cell bodies receive input from other central nuclei in primates and so shed light on the roles Mes V plays in human mastication.

Materials and methods

These experiments were undertaken in five young adult (3.0–5.0 kg) *Macaca fascicularis* monkeys, of which three were male and two were female. The surgical procedures were approved by the University of Mississippi Medical Center Institutional Animal Care and Use Committee, and fell within the National Institutes for Health guidelines governing research on animals. Animals were housed in an AAALAC approved facility. In two macaques, intramuscular injections of a combination of 1% wheat germ agglutinin conjugated to horseradish peroxidase (WGA-HRP) and 10% horseradish peroxidase (HRP) were placed in the masseter and lateral pterygoid muscle. These animals were initially sedated with ketamine HCl (10 mg/kg, i.m.) and then anesthetized with isoflurane (1–3%). They received atropine sulfate (0.05 mg/kg, i.v.) to control excess secretions. A 10 µl Hamilton syringe was used to inject 10 µl of the WGA-HRP/HRP mixture into the left masseter and right lateral pterygoid muscles. These two animals and the other three animals received a central injection of another tracer for a different study at sites that would not affect the results of this Mes V study. Following surgery, buprenex (0.01 mg/kg, i.m.) was given to avoid postoperative discomfort. After allowing appropriate time for tracer transport (48 h), all animals were sedated with ketamine HCl (10 mg/kg, i.m.) and were then given sodium pentobarbital (50 mg/kg, i.p.) to induce deep anesthesia. Once insensate, they were perfused through the heart with buffered saline, followed by a mixture of 1.25% paraformaldehyde and 2.0% glutaraldehyde in 0.1 M, pH 7.2 phosphate buffer. The brains were blocked in the frontal plane, extracted and post-fixed for ~ 1 h in the same paraformaldehyde/ glutaraldehyde solution, then stored in 0.1 M, pH 7.2 phosphate buffer at 4 °C.

The brainstems of these specimens were cut into 100 µm thick frontal sections on a Leica VT1000S vibratome (Leica Biosystem, Wetzlar, Germany), and the sections were collected as an ordered series in 0.1 M, pH 7.2 phosphate buffer. To reveal the HRP, sections were incubated in tetramethylbenzidine (TMB) using the method of Olucha and colleagues (Olucha et al. 1985; Perkins et al. 2009). An ordered 1 in 3 series of sections was first placed in a 0.005% solution of TMB dissolved in 0.1 M, pH 6.0 phosphate buffer with 0.25% ethanol and 0.245% ammonium molybdate. Then the reaction was initiated with 0.011% H_2O_2 and ran at 4 °C for ~ 12 h. Following stabilization in 5.0% ammonium molybdate, sections were rinsed in the buffer, mounted on gelatinized slides, dried, counterstained with cresyl violet, dehydrated in ethanols and cleared in toluene for light microscopy.

For electron microscopy, a second ordered 1 in 3 series was reacted as above, then the TMB reaction product was further stabilized by reacting the tissue in a solution of 5% diaminobenzidine (DAB) dissolved in 0.1 M, pH 7.2 phosphate buffer. Once again, the reaction was initiated with 0.011% H_2O_2. Free floating sections were examined with a Wild M8 stereomicroscope (Leica Biosystem, Wetzlar, Germany), and small blocks that contained labeled neurons were

taken from the region along the edge of the periaqueductal gray. We examined two labeled cells in one of the injected cases and three labeled cells in the other injected case. In the case of the animals without muscle injections, this same region was examined and samples were taken that contained the large diameter, presumed Mes V neurons. These were then prepared for electron microscopy (Wang and May 2008; Barnerssoi and May 2015). The samples were osmicated in 1.0% OsO_4 dissolved in 0.1 M, pH 7.0, phosphate buffer and *en block* stained in 2.0% uranyl acetate. They were dehydrated and embedded in Durcupan using conventional techniques, before semi-thin sections were cut. The semi-thin (1 µm) sections were placed on slides and stained with toluidine blue. These were used to guide further trimming of the blocks. Then ultrathin (silver–gold) sections were cut on a Leica Ultracut UCT (Leica Biosystem, Wetzlar, Germany) equipped with a diamond knife and collected onto copper grids. These were stained with lead citrate before being examined on a Zeiss (Carl Zeiss Microscopy, White Plains, NY) or JOEL (JOEL USA, Inc, Peabody, MA) transmission electron microscope. A total of 17 blocks containing Mes V neurons (4 blocks containing Mes V cells per non-retrogradely labeled animal) were examined in this way. Light microscopy was done with a Nikon Eclipse E600 microscope equipped with a Nikon DXM 1200F digital camera (Nikon Instruments, Inc, Mellville, NY).

Results

Following injections of either the masseter muscle or lateral pterygoid muscle, scattered cells were labeled within the mesencephalic trigeminal nucleus (Mes V). An example is shown in Fig. 1A, B. The labeled neurons (Fig. 1B, arrowhead) were characterized by the dark brown reaction product within their somata. Labeled motoneurons were also present in the trigeminal motor nucleus indicating a masticatory muscle had been injected. Labeled Mes V neurons like these were located along the edge of the periaqueductal gray, but were much larger than the neurons found within the substance of the periaqueductal gray or immediately outside its borders. Unlabeled cells with similar sized somata, presumed Mes V neurons, were also arrayed along the edge of the periaqueductal gray. These were arranged both singly and in small groups (Fig. 1B, C). They displayed a single prominent nucleolus within a large euchromatic nucleus. The cytoplasm was densely studded with Nissl bodies. Samples that contained labeled cells were taken for electron microscopy in the two animals with muscle injections, but relatively few labeled cells were present. Consequently, using the location and large somal characteristics, we were able to more widely sample the Mes V population in the three animals that had not received muscle injections. An example of the presumed Mes V cells in an unlabeled animal is shown in Fig. 1C. Note how the Mes V neurons are much larger than adjacent neurons of the periaqueductal gray (arrowheads). An example of a region sampled for electron microscopic study is shown in Fig. 1D.

Figure 2 shows an electron microscopic view of an example of a retrogradely labeled Mes V cell (Soma*) from an animal that received muscle injections. In this case, the cell was labeled from a lateral pterygoid muscle injection. Electron dense reaction product fills the cytoplasm in this case, making it hard to appreciate the cytoplasmic contents, although electron dense vacuoles can be observed. No synaptic terminals were observed contacting this labeled somatic profile. The reaction product was also present within spinous extensions (Sp*) of the soma. The examples shown (Fig. 2B) are adjacent to an axon terminal (At) that contains small spherical clear vesicles and a few dense-cored vesicles (arrows). No synaptic densities were present between these elements. The majority of the associations between vesicle filled profiles and somata or their spines were like this one, in that they lacked a clear synaptic density between the two elements.

Figure 3A shows another example of a retrogradely labeled Mes V neuron (Soma*) from the second animal. The cytoplasmic staining was distinctly lighter in this example, which is again characterized by electron dense vacuoles (arrows). A large region containing stacks of rough endoplasmic reticulum (rER) is present at the lower left and the cytoplasm between the polyribosomes is also electron dense, indicating that the cell is labeled (Fig. 3B). Despite its extensive perimeter, only a single synaptic contact was observed along its plasma membrane in this section (Fig. 3B). Glial processes can be observed in contact with the somatic membrane on either side of the synapse. In this axon terminal (At), the vesicles appeared to be clear and pleomorphic. The synaptic density (arrowhead) was slightly asymmetric. Note that the vesicles were not particularly associated with the synaptic density. Of the Mes V neuron profiles examined, 52.4% (43/82) showed an association in which vesicle filled profiles had membranes contiguous with either the somatic membrane or its spines. A minority of these displayed synaptic densities like this one that connected the profile to the Mes V neuron.

The nucleus of a presumed Mes V neuron, which comes from a retrograde labeling case, is quite large and euchromatic, with a prominent nucleolus (Fig. 4). The soma itself is also quite large (> 50 µm) and has a cytoplasm filled with the usual compliment of rER and mitochondria. The cytoplasm does not show any evidence of retrograde labeling, although it still contains a large contingent of vacuoles (arrows). These are heterogeneous with both electron dense and electron lucent components. The common presence of these vacuoles in Mes V cell bodies may be related to the large

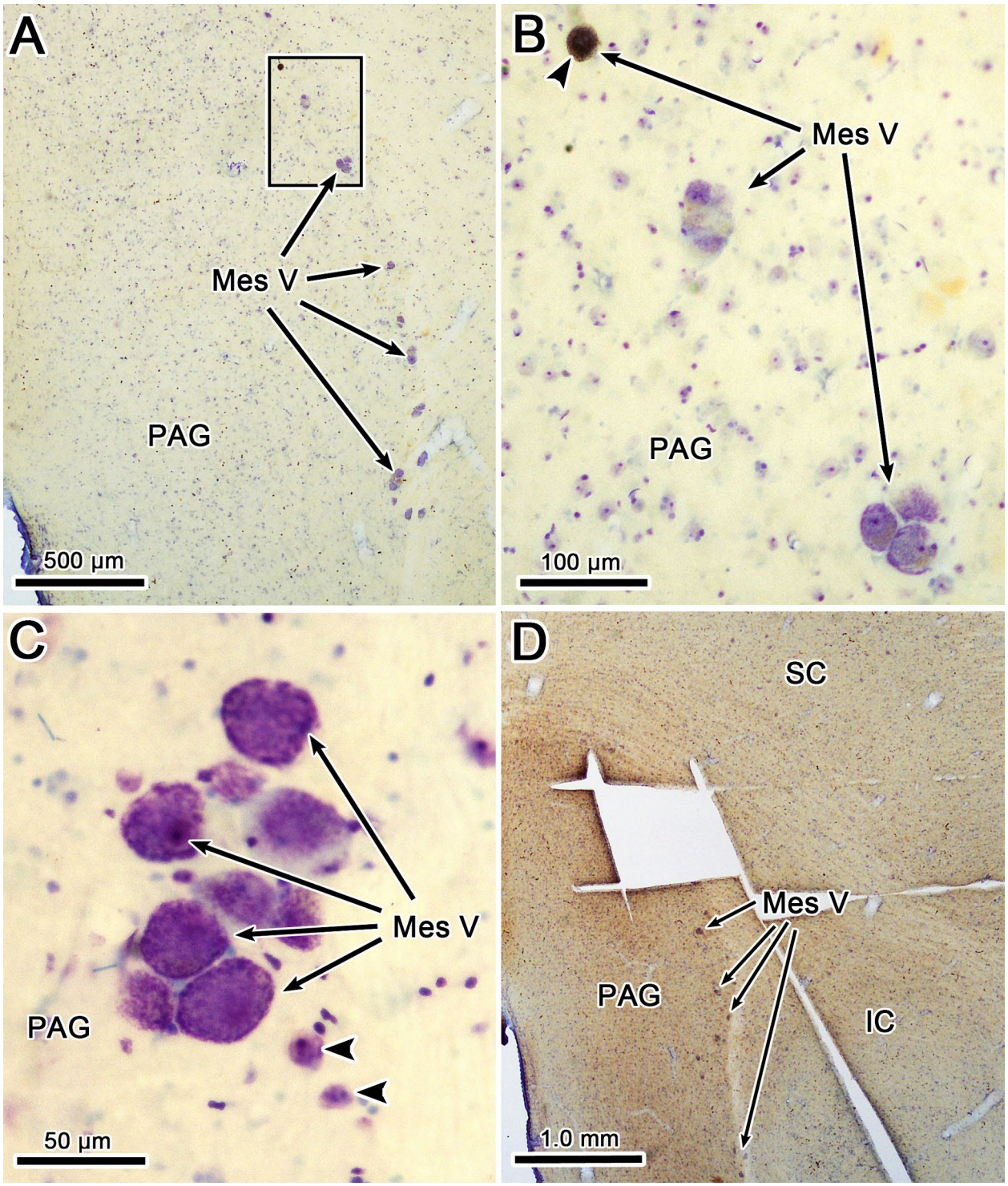

Fig. 1 Light microscopic view of mesencephalic trigeminal nucleus (Mes V). **A** Due to their large size, Mes V cells are readily apparent along the edge of the PAG. Boxed area is shown at higher magnification in **B**, where the retrogradely labeled cell (arrowhead) is labeled by dark reaction product, in contradistinction to the cresyl violet label clusters of Mes V cells. **C** A higher magnification view of a cluster of counterstained Mes V neurons from an animal that did not receive muscle injections. Note their large size relative to the two neurons (arrowheads) belonging to the PAG. **D** Example of block taken for electron microscopy. Although these samples also include portions of the adjacent, PAG, SC or IC, further trimming removed much of these non-relevant areas. *At* axon terminal, *Ax* axon, *Den* dendrite, *IC* inferior colliculus, *Mes V* mesencephalic trigeminal nucleus, *Nu* nucleus, *PAG* periaqueductal gray, *rER* rough endoplasmic reticulum, *SC* superior colliculus, *Soma** labeled cell body, *Sp* spine, *Sp** labeled spine

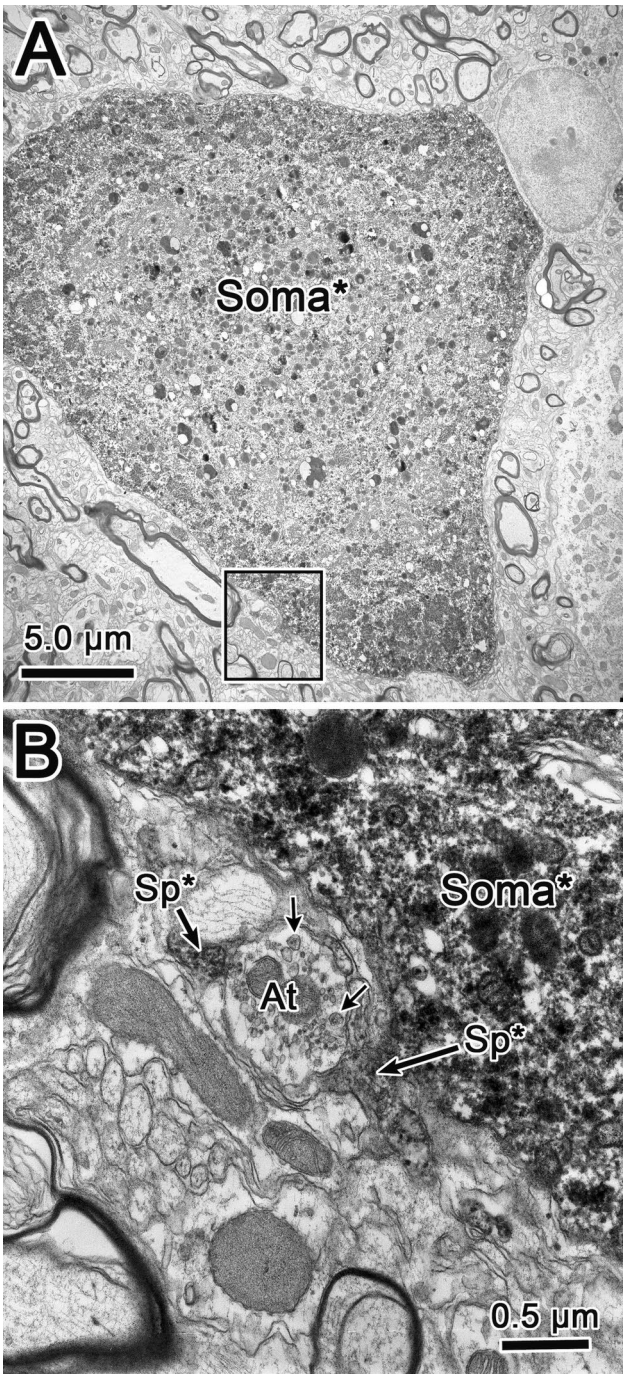

Fig. 2 Ultrastructure of a retrogradely labeled Mes V neuron. **A** The retrogradely labeled soma (Soma*) was characterized by a diffusely electron dense cytoplasm. It was quite large and displayed numerous vacuoles with electron dense reaction product. The boxed region is shown at higher magnification in **B**. Labeled spines (Sp*) containing electron dense reaction product are shown in **B**, where they are adjacent to an axon terminal (At) that contains clear spherical vesicles and a few dense-cored vesicles (arrows). No synaptic density indicating contact between the terminal and the spines was observed

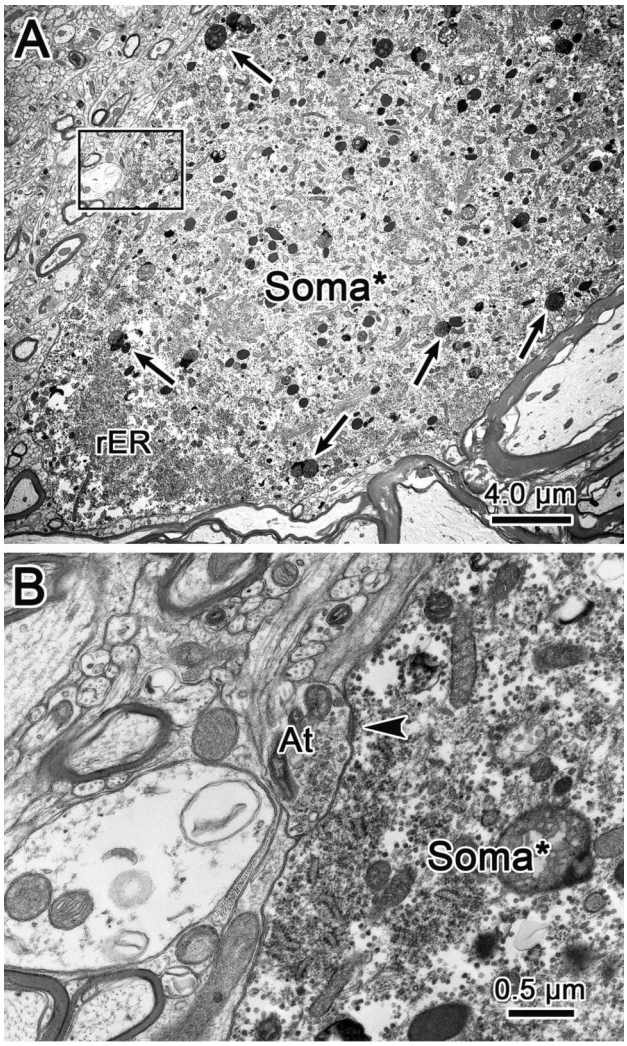

Fig. 3 Synaptic contact on a retrogradely labeled Mes V neuron. **A** Less electron dense reaction product is present in the cytoplasm of this soma (Soma*) compared to that shown in Fig. 2. It also displays electron dense vacuoles (arrows) and stacks of rough endoplasmic reticulum (rER). Box indicates region shown in **B**, where an axon terminal (At) displays a synaptic density (arrowhead) where it contacts the somatic membrane. Note the increased electron density of the cytoplasm between the polyribosomes, indicative of retrograde labeling. The terminal contains clear, pleomorphic vesicles

metabolic load that these neurons, with their large somata and extensive axonal arbors, need to support. An appreciation of the size of these cells can be obtained by comparison to the neuron in the upper right (Soma). This cell has a small soma (< 20 µm) and is quite typical of the non-Mes V neurons found in the samples. To appreciate their relative sizes, note that this entire neuron would fit within the nucleus of the Mes V cell. Due to the unusual arrangement of the Mes V cells at the edge of the periqueductal gray, our samples inevitably contained cell bodies and other profiles that may or may not be part of the Mes V nucleus. For this reason,

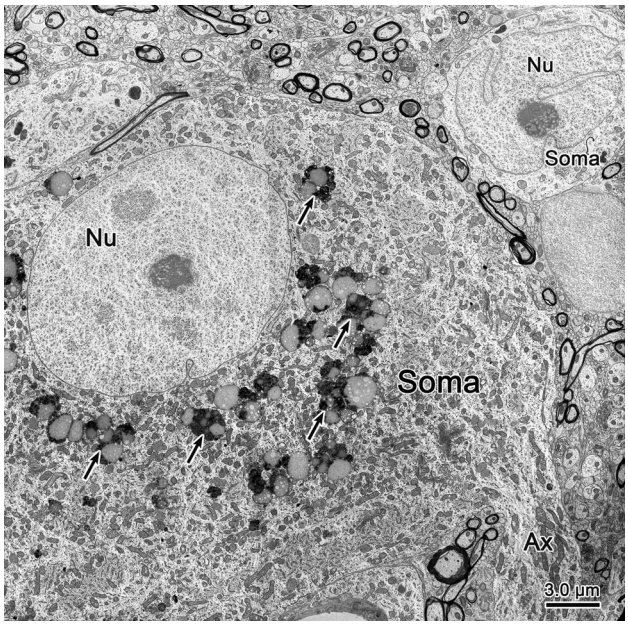

Fig. 4 Ultrastructure of an unlabeled Mes V neuron. The soma (Soma) of this neuron is quite large. The nucleus (Nu) of this neuron is large and euchromatic with a prominent nucleolus. Numerous vacuoles (arrows) with complex heterogeneous electron density cluster around the nucleus. A thick axon (Ax) emerged from the soma. An adjacent neuron with a much smaller soma (Soma, upper right) provides a ready contrast with the Mes V cell

we concentrated on the large somata that belong to Mes V. A single thick axon (Ax) (diameter ~ 8 µm) extends from the soma of the Mes V neuron. No contacts were observed on the somatic membrane of this Mes V neuron example or its axon. This was the case for 47.6% (39/82) of the somatic profiles investigated. On the other hand, multiple axosomatic synaptic contacts were present on examples of smaller neurons found in the vicinity of the Mes V cells (not illustrated).

Figure 5 shows a cluster of presumed Mes V neurons from an unlabeled case. The cell cut through the nucleus has a diameter ~ 45 µm, and the nucleus is both large and euchromatic. The other two profiles, which lack nuclei, were designated as somata as they shared similar characteristics, including large diameter in the case of the middle cell and stacks of rER and heterogeneous vacuoles in the case of both profiles. One of the common features observed on Mes V neurons is shown here: somatic spines of varying lengths (Fig. 5B-D). Some prospective spines are merely bumps on the somatic surface, but this appearance may be due to the plane of section. These are not like the spines found in cortices with narrow necks leading to broader heads. Instead, they are narrow, often curving, processes that extend from the somatic membrane for a short distance. They extend into the neuropil surrounding the soma and are occasionally associated axon terminals (At) (Fig. 5C), but are more often not associated with them (Fig. 5B and D). Note that there is no evidence of a synaptic density in Fig. 5C, but one synaptic contact (arrowhead) was observed on the Mes V cell's somatic membrane (Fig. 5E). This small terminal displayed a short asymmetric contact and clear spherical vesicles, although the lack of clustering of the vesicles adjacent to the density may indicate that this is a punctum adherens. Axon terminals are often present beside the somatic membranes (Fig. 5B and C) and spinous membranes (Fig. 5B–D), but do not display a synaptic contact linking them. Similarly, in some cases, synaptic contacts were observed on small profiles that are likely spines, but the connection of the postsynaptic profile to the Mes V soma could not be verified (Fig. 5D). Details of a presumptive Mes V axon (shown in Fig. 5A, lower left) are shown in Fig. 6. We believe this is an axon belonging to a Mes V neuron based on its similarity to the axon extending from the somata in Fig. 5, including its large diameter (~ 7 µm) and similarity to other axons observed extending from other somata in our material (Supplemental Fig. 1A). The axon dwarfs the adjacent myelinated axons. This is presumably a connecting process that extends to the point where the myelinated peripheral and central processes join. Its large diameter would lessen its resistance, allowing action potentials to access the soma or graded synaptic potentials to reach the place where the three processes meet. What is even more striking is the size of many of the mitochondria (arrows) present within this profile. Some are more than a micron across. Larger mitochondria have been observed at nodes of Ranvier and within initial segments, as these areas may require more energy for ion pumps (Dimova and Markov 1976; Ohno et al. 2011). Perhaps the large diameter connecting processes of Mes V axons also require greater amounts of chemical energy.

Further examples of the neuropil seen adjacent to the Mes V somatic membranes are shown in Figs. 7 and 8. The numerous and varied somatic spines present on these cells are demonstrated in Fig. 7A–C. Note that while these spinous processes are often adjacent to axon terminals (At), synaptic densities were rarely encountered. In Fig. 7A, the terminal contacts (arrowhead) another small profile, not the spine. In Fig. 7B, a small synaptic density (arrowhead) indicates contact with the somatic membrane, not the spine. One can also see an example of the glial processes that often enveloped the somatic membrane in the region between spines in Fig. 7B. Within clusters of Mes V cells, the spines of adjacent cells often displayed non-synaptic relationships (Fig. 7C; Supplemental Fig. 1B). One of the uncommon examples of a well formed axosomatic contact is shown in Fig. 8. This Mes V neuron showed deep invaginations of the nuclear envelope (Fig. 8A). This was not uncommon in these cells. In this case, the clear pleomorphic vesicles in the terminal are clustered around a symmetric synaptic density (arrowhead) on the plasma membrane of the soma (Fig. 8B).

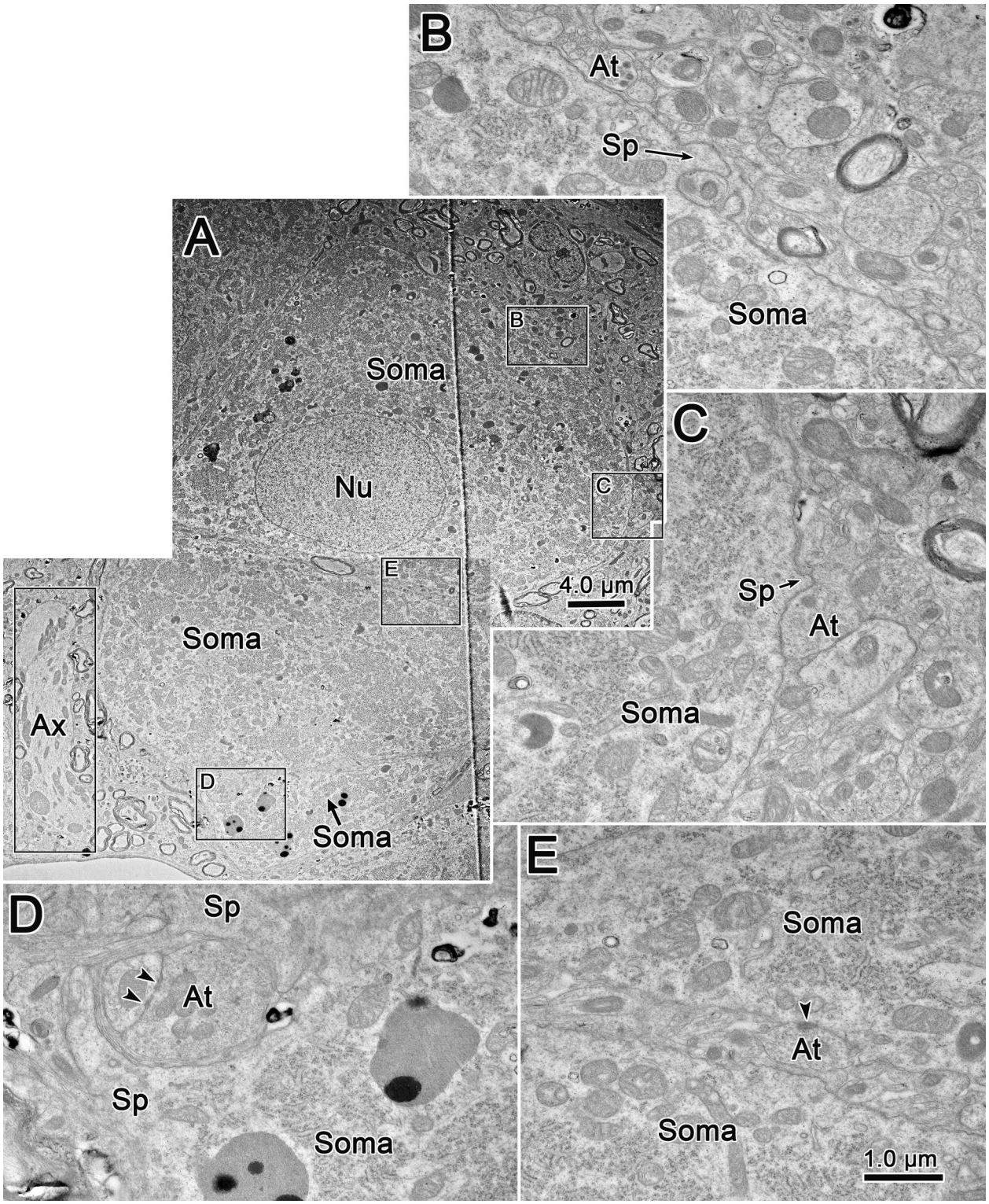

Fig. 5 Somatic spines (Sp) characterize Mes V neurons. **A** Three unlabeled Mes V neurons are characterized due their large somata (Soma) and large euchromatic nuclei (Nu). Lettered boxes indicate location of other plates. **B**–**D** Numerous and varied spinous processes extend from the somatic membrane, but no synaptic contacts (arrowhead) from adjacent axon terminals (At) are evident on these spines. **E** A small axosomatic contact was observed on one of the Mes V neurons. Boxed area containing an axon (Ax) at left of **A** is shown in Fig. 6. Scale in **B**–**D** shown in **E**

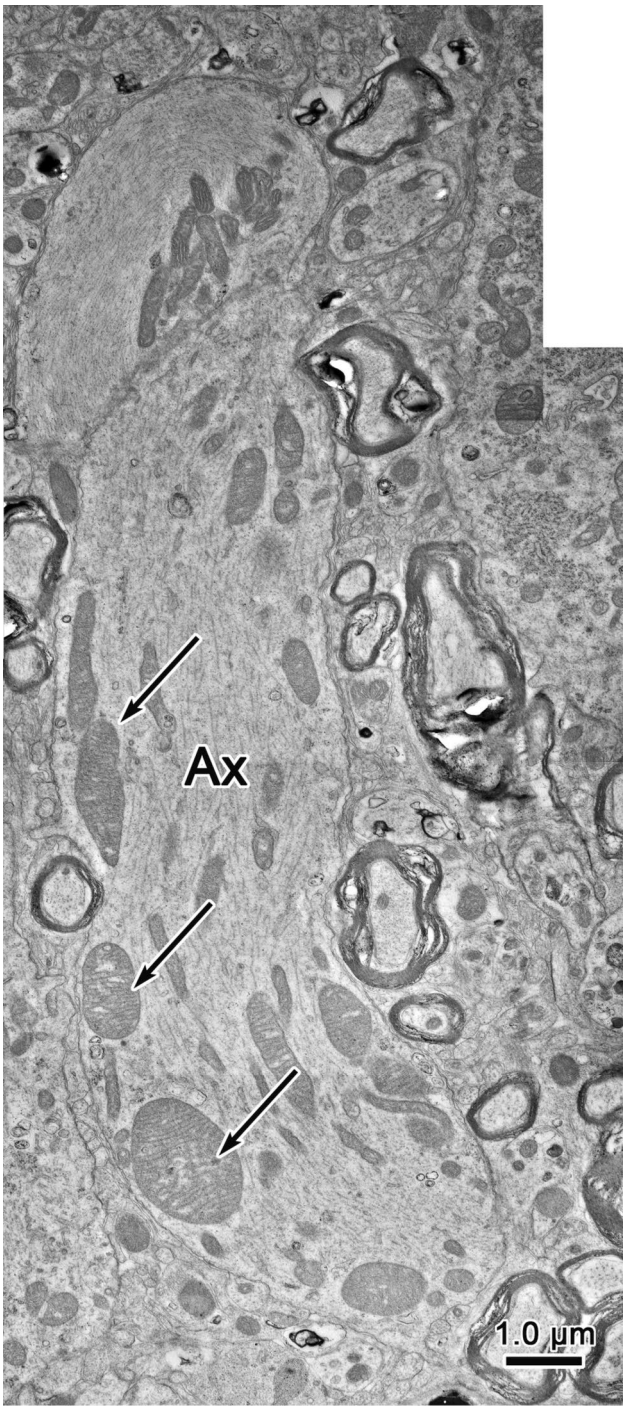

Fig. 6 Presumptive Mes V neuron axon (Ax). Very large axons like the one shown here were often associated with the clusters of Mes V somata. An unusual characteristic of these axons was the presence of very large mitochondria (arrows)

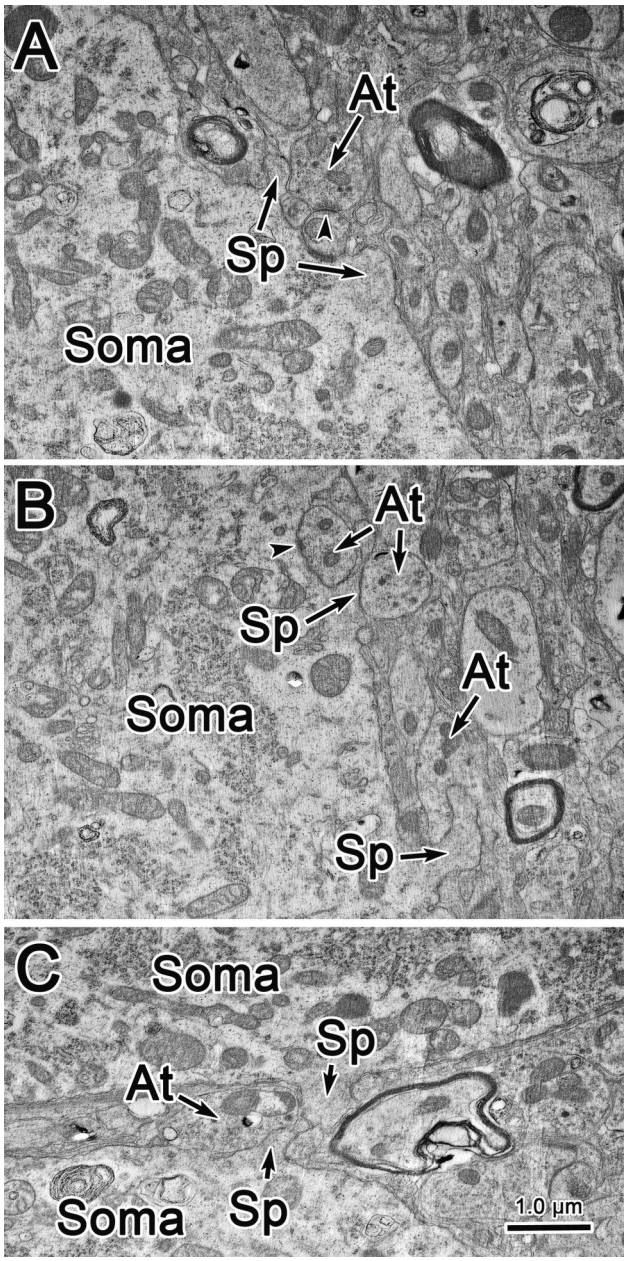

Fig. 7 Perisomatic neuropil of Mes V neurons. **A** Two short spines (Sp) extend from the soma (Soma) of the cell near a vesicle containing axon terminal (At), but it does not contact either, and instead displays a synaptic density (arrowhead) on another small process. **B** Two longer somatic spines are associated with axon terminals, but these display no synaptic densities. A synaptic contact with the soma is present, however. **C** Spines from adjacent somata have plasma membranes that are in contact, but no synaptic contact is seen with the adjacent axon terminal. Scale in **A** and **B** shown in **C**

While axon terminals with clear synaptic contacts are quite rare on the somatic membranes of Mes V cells, it is possible that these cells have dendrites that receive synaptic contact. We did not generally observe dendrites extending from the Mes V cell bodies of our macaque monkey samples. Figure 9 shows the one case we observed where such a dendrite may be present. In this case, only a portion of the soma was present, so we could not be absolutely certain this was a Mes V somata. However, it was adjacent to two other large somatic profiles and it displayed similar

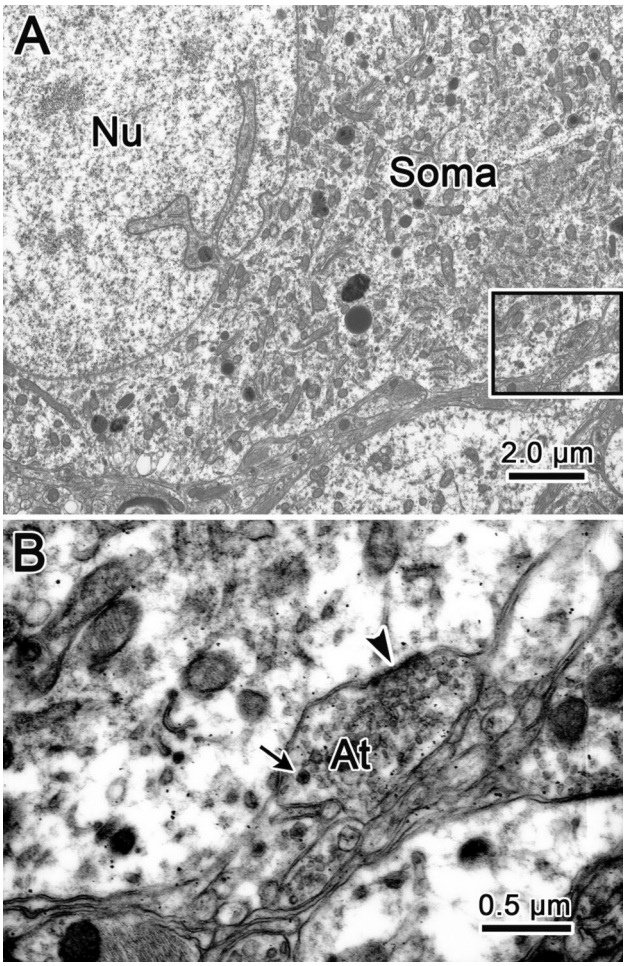

Fig. 8 Axosomatic contact on presumed Mes V neuron. **A** shows a typical Mes V neuron (Soma) whose euchromatic nucleus (Nu) has a deeply indented nuclear envelope. Boxed area is shown in **B**, where an axon terminal (At) with clear pleomorphic vesicles and a single dense-cored vesicle (arrow) displays a slightly asymmetric synaptic density (arrowhead) that contacts the somatic plasma membrane

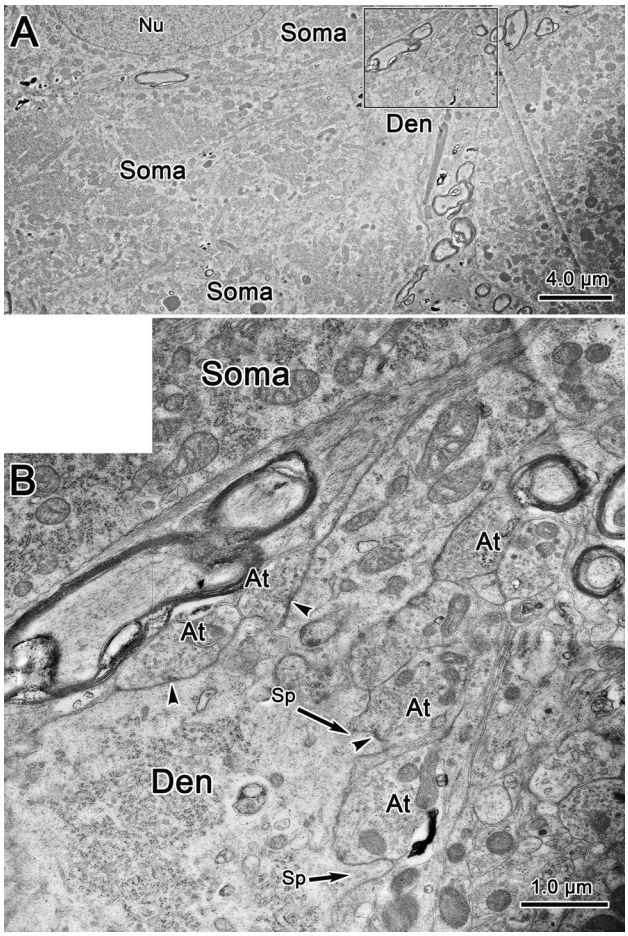

Fig. 9 Terminals contacting putative Mes V dendrite. **A** A cluster of presumed Mes V somata (Soma) containing three neurons, with one showing a euchromatic nucleus (Nu). At the bottom, a tangential profile of a soma displays a dendrite. The boxed area shown at higher magnification in **B** reveals the presence of multiple axon terminals (At) making synaptic contact (arrowhead) with this dendrite or the short spinous processes (Sp) that extended from it

ultrastructural characteristics to the adjacent Mes V somata, that is a large diameter and stacks of rER (Fig. 9A). This presumptive Mes V dendrite tapered from the somatic profile as is typical of dendrites. Furthermore, it lacked the stacks of rER of somata and it showed a much higher incidence of synaptic contact by axon terminals than was observed on somatic membranes (Fig. 9B). The dendrite also displayed a number of spinous processes, some of which were postsynaptic (arrowheads) to axon terminals (Fig. 9B).

Discussion

In the present study, we first confirmed the location of Mes V neurons by retrograde labeling from the masticatory muscles in macaque monkeys. Ultrastructurally, these neurons have very large somata containing large, euchromatic nuclei. Compared to the adjacent cell bodies, which were distinctly smaller in size, the plasma membranes of these Mes V somata were largely devoid of synaptic contact. They did extend numerous somatic spines of various lengths into the neuropil, but most of these spines lacked synaptic contacts as well. The small number of terminals observed contacting Mes V somata displayed varied vesicle and synaptic density characteristics. Taken together, these ultrastructural features provide support for the hypothesis that primate Mes V cell bodies do receive direct synaptic input from various central nuclei. So the masticatory information from muscle spindles and periodontal ligament receptors that is transmitted by Mes V cells can be modified by axosomatic input from other central nuclei. On the other hand, the present results suggest this is a rather limited central input in macaques.

Of the 82 Mes V somatic profiles examined, 43 (52.4%) displayed plasma membranes where axon terminals were in contact with it or its spines and 39 (47.6%) showed no such contacts. Of the former group, less than half demonstrated a clear postsynaptic density proving that the association was indeed synaptic. Those cell bodies with synaptic contacts very rarely displayed more than one such input.

Technical considerations

The strength of the ultrastructural data presented here is limited by the relatively small sample size, compared to previous ultrastructural studies undertaken in rodents and cats (cat: Lazarov 1996; Honma et al. 2001; rat: Liem et al. 1991; Liem et al. 1992; Paik et al. 2005). Nevertheless, the fact that the findings are quite similar to those previously seen in non-primates suggests that not only are the results valid, they are probably applicable to the human Mes V as well. While the majority of the cells we analyzed were not retrogradely labeled, the clear similarities with respect to soma size and ultrastructural characteristic between the labeled and unlabeled samples leave us confident that the appropriate neurons were analyzed. We only retrogradely labeled muscle spindle afferents and only examined cells along the border of the periaqueductal gray, so it is possible that periodontal afferents and Mes V neurons adjacent to the locus coeruleus might display different characteristics. Examining this possibility will require additional studies.

Comparison to previous studies

We did not divide the axon terminals into different subclasses or quantify the occurrence of different types. This was due to the fact that our sample of axon terminals with clear synaptic termination onto Mes V somata ($n = 20$) was too small to justify making such classifications or quantification. However, it was apparent that profiles with both round and pleomorphic clear vesicles were present, as well as ones that also contained a few small dense-cored vesicles. Furthermore, both symmetric and modestly asymmetric synaptic densities were observed. We also saw a couple of examples of profiles dominated by large dense-cored vesicles, but as no synaptic contacts were visible, we have not illustrated them. Thus, our findings mirror those seen in non-primate species where a variety of synaptic types have been recognized, classified, and quantitatively studied (cat: Lazarov 1996; Honma et al. 2001; rat: Liem et al. 1991; Liem et al. 1992). One noteworthy feature is that the conventional pairing of round vesicles and asymmetric contacts was not always observed. This may be due to the fact the cut was not through the middle of the synapse, or it could indicate that non-conventional synaptic types are present in Mes V. In a general sense, the presence of varied synaptic morphology suggests that there is more than one type of input influencing Mes V activity. We did not specifically look for electrotonic junctions between Mes V somata, although such coupling has been reported in rodents (Hinrichsen 1970; Baker and Llinas 1971; Curti et al. 2012). We rarely saw somatic membranes lying immediately adjacent to each other, but the extensive interaction between spines of adjacent cells may offer a site for such interaction (Supplemental Fig. 1B).

Mes V neuron ultrastructure in macaque monkeys shows a lot of similarities to that observed in other animals, such as rats (Liem et al. 1991; Paik et al. 2005) and cats (Honma et al. 2001). In all species studied to date, Mes V neurons have large somata with numerous spines, a large euchromatic nucleus, and abundant rER (Lazarov 2000). Our study did not find as many axosomatic synapses on macaque monkey Mes V somata as has been reported for non-primate cell bodies (rat: Liem et al. 1992; cat: Lazarov 2000), although Liem and colleagues (1991) suggest that only 4–5 contacts are present per 100 µm of somatic perimeter in rats, which is still a low level of coverage. This difference in the primate findings could be caused by the limited sample size, or could represent a true species difference. In all species examined to date, most of the synapses were present on dendrites, not the somata, despite the extensive areas of somatic plasma membrane available (cat: Lazarov 1996; Lazarov 2000; Honma et al. 2001; rat: Liem et al. 1991; Liem et al. 1992). In the present study, only one example of a dendrite that was clearly in continuity with a presumptive Mes V soma was observed. Like the dendrites examined in non-primate studies, it displayed a much higher degree of synaptic coverage suggesting dendrites are the major locations to receive inputs. How common such dendrites are on Mes V neurons is still a matter of debate (Nomura et al. 1985; Lazarov 2000). The fact that we only observed one putative dendrite in our samples suggest that they may be relatively rare in macaques, but further examination of this point is required.

Another unusual characteristic observed here was the presence of large diameter axons extending from (Fig. 4) or in the vicinity (Fig. 5) of the cell bodies. These connecting processes are at least initially unmyelinated, in contradistinction to the central and peripheral processes (Luo and Li 1991). Similar axonal processes have been observed in other species (Honma et al. 2001) and they occasionally receive synaptic contacts. Only one example of such an axoaxonic contact (not illustrated) was seen in the present material, but our sample was quite small.

In contrast to the sparse axosomatic synapses observed on labeled and unlabeled Mes V somata, we found many axosomatic synapses on smaller neurons in the neuropil adjacent to Mes V cells (not illustrated). This may suggest that information from other central structures could be relayed by interneurons adjacent to the primary afferent somata before it reaches Mes V. In other words, central input could

be modified and integrated through interneurons (Luo et al. 1991; Yoshida and Oka 1998). However, it is equally possible that these cells are just part of the general population within the periaqueductal gray, and their location adjacent to Mes V neurons does not indicate they are part of the masticatory circuitry.

Functional considerations

The peripheral arms of Mes V axons receive proprioceptive information from muscles spindles of masticatory muscles and mechanoreceptors within the periodontal ligament, and the central arms transmit this signal directly and indirectly to trigeminal motoneurons that control the rhythmic contraction of muscles during mastication. As such, they subserve masticatory reflexes. Mes V central axons also project to other motor nuclei, including the hypoglossal nuclei, and even to the cervical spinal cord (cat: Bae et al. 1996; Yabuta et al. 1996; Kishimoto et al. 1998; rat: Luo and Li 1991; Luo et al. 1991; Bae et al. 2018). These motor nuclei receive feedback from the masticatory apparatus through these Mes V projections so that muscles in the tongue, face, and neck can cooperate during mastication, swallowing, and speech. The presence of synaptic input, as observed here, suggests that the activity in all these projections of macaque Mes V neurons is also regulated by higher level central nuclei, possibly including the reticular formation, raphe nuclei, substantia nigra, amygdala, hypothalamus, and habenula (rat: (Luo et al. 1991; Liem et al. 1997; Dessem and Luo 1999; Iida et al. 2010; Takahashi et al. 2010; Lazarov et al. 2011; Shirasu et al. 2011; Ohara et al. 2016). These central synaptic inputs to Mes V neurons likely provide a morphological substrate whereby the behavior of mastication is significantly influenced by learning, memory, and diverse emotions such as stress and anxiety. These emotional factors likely play a role in changing activity levels in the masticatory circuitry for pathologies such as bruxism and temporomandibular joint disorder (Ishii et al. 2005, 2006; Mascaro et al. 2009; Takahashi et al. 2010; Shirasu et al. 2011; Espana and Clotman 2012; Ohara et al. 2016; Liu et al. 2017, 2019; Giovanni and Giorgia 2021; Zhao et al. 2022). There is also evidence from rodent studies that Mes V neurons receive intrinsic feedback from their own axon collaterals and from GABA positive neurons within Mes V (rat: Luo and Dessem 1996; Dessem and Luo 1999; Yokomizo et al. 2005). The unique central location of Mes V neurons, which distinguishes them from other primary afferent neurons located in dorsal root and trigeminal ganglia, facilitates their diverse central inputs and projections. Although Mes V plays a crucial role in supplying peripheral information in mastication, the sources of central input to these primary afferent neurons and the types of influence produced by central nuclei remains to be determined in primates. Certainly, the presence of numerous synaptic profiles in the perisomatic neuropil of Mes V neurons that do not appear to actually contact the Mes V somata should give pause. Inferring synaptic input solely based on close associations between Mes V somata and labeled terminals using light microscopic analysis, such as we did previously (Wang and May 2008), should be approached with great caution.

In light of the presence of synaptic input, the question of whether the flow of proprioceptive information from the periphery can be modified in the Mes V system needs to be addressed. Normally, action potentials move directly from the peripheral process to the central process in pseudounipolar neurons. The soma and its connecting axon mainly perform a nutritive support function for the rest of the axon. The flow of action potentials from the peripheral to central process could only be influenced by central synapses if there was a high likelihood of branch point failure where the peripheral, central, and connecting processes meet, or if action potentials could be produced at the initial segment that caused collision with incoming action potentials. In both cases, one would expect that synapses would be clustered on the soma, closer to the trifurcation, as opposed to on the dendrites, to be in a position to maximally affect action potentials transmitted from the periphery. Furthermore, collision would require precise timing to be effective, and this is an unlikely scenario. It may make more sense to consider that Mes V cell bodies have a central location for reasons other than to allow modulation of incoming proprioceptive signals. For example, it has been suggested that this location is due to the fact that a true jaw developed later than the rest of the segmental somatic apparatus (Sato 2021). Nevertheless, the presence of synapses on these neurons may indicate that other nuclei have simply taken advantage of the central location of Mes V somata to provide a convenient way to influence Mes V targets and the act of mastication by synaptically initiating their own action potentials at the Mes V neuron initial segment. This interpretation of synaptic function would help explain why synaptic effects have not been found to modify the jaw stretch reflex (De Montigny and Lund 1980).

Supplementary Information The online version contains supplementary material available at https://doi.org/10.1007/s00221-023-06746-y.

Acknowledgements We wish to acknowledge the help of Jayne Bernanke, Glenn Hoskins, and Jeremy Sullivan in the ultrastructural preparation of tissues. In addition, we thank Susan Warren, PhD for helpful comments on earlier drafts of this manuscript.

Author contributions Experimental design, surgical procedures and figure production: PJM. Ultrastructural analysis, writing and editing: NW and PJM.

Funding This work was supported by the National Institutes of Health [grant number EY014263] to PJM.

Data availability The electron micrographs that formed the basis for this study are available for examination by request to the authors.

Declarations

Conflict of interest The authors have no conflicts of interest, financial or otherwise, with respect to the publication of this manuscript.

Ethical use of animal statement All applicable international, national, and/or institutional guidelines for the care and use of animals were followed. All procedures performed in studies involving animals were in accordance with the standards of the institution at which the studies were conducted. Specifically, they were undertaken under protocols approved by the Institutional Animal Care and Use Committee of the University of Mississippi Medical Center (USDA Animal Welfare Assurance # D16-00174) and housed in an AAALAC accredited facility.

Generative AI and AI-assisted technologies in the writing process The authors did not use artificial intelligence in the analysis of the data or the production of this manuscript.

References

Bae YC, Nakagawa S, Yasuda K et al (1996) Electron microscopic observation of synaptic connections of jaw-muscle spindle and periodontal afferent terminals in the trigeminal motor and supratrigeminal nuclei in the cat. J Comp Neurol 374:421–435. https://doi.org/10.1002/(SICI)1096-9861(19961021)374:3%3c421::AID-CNE7%3e3.0.CO;2-3

Bae JY, Lee JS, Ko SJ et al (2018) Extrasynaptic homomeric glycine receptors in neurons of the rat trigeminal mesencephalic nucleus. Brain Struct Funct 223:2259–2268. https://doi.org/10.1007/s00429-018-1607-3

Baker R, Llinas R (1971) Electrotonic coupling between neurones in the rat mesencephalic nucleus. J Physiol 212:45–63. https://doi.org/10.1113/jphysiol.1971.sp009309

Barnerssoi M, May PJ (2015) Postembedding immunohistochemistry for inhibitory neurotransmitters in conjunction with neuroanatomical tracers. In: Van Bockstaele E (eds) Transmission electron microscopy methods for understanding the brain. Neuromethods, vol 115. Humana Press, New York, NY. pp 181–203. https://doi.org/10.1007/7657_2015_79

Byers MR, O'Connor TA, Martin RF, Dong WK (1986) Mesencephalic trigeminal sensory neurons of cat: axon pathways and structure of mechanoreceptive endings in periodontal ligament. J Comp Neurol 250:181–191. https://doi.org/10.1002/cne.902500205

Capra NF, Anderson KV, Atkinson RC 3rd (1985) Localization and morphometric analysis of masticatory muscle afferent neurons in the nucleus of the mesencephalic root of the trigeminal nerve in the cat. Acta Anat (basel) 122:115–125. https://doi.org/10.1159/000145992

Chen P, Li J, Li J, Mizuno N (2001) Glutamic acid decarboxylase-like immunoreactive axon terminals in synaptic contact with mesencephalic trigeminal nucleus neurons in the rat. Neurosci Lett 298:167–170. https://doi.org/10.1016/s0304-3940(00)01736-5

Curti S, Hoge G, Nagy JI, Pereda AE (2012) Synergy between electrical coupling and membrane properties promotes strong synchronization of neurons of the mesencephalic trigeminal nucleus. J Neurosci 32:4341–4359. https://doi.org/10.1523/JNEUROSCI.6216-11.2012

De Montigny C, Lund JP (1980) A microiontophoretic study of the action of kainic acid and putative neurotransmitters in the rat mesencephalic trigeminal nucleus. Neuroscience 5:1621–1628. https://doi.org/10.1016/0306-4522(80)90026-3

Dessem D, Luo P (1999) Jaw-muscle spindle afferent feedback to the cervical spinal cord in the rat. Exp Brain Res 128:451–459. https://doi.org/10.1007/s002210050868

Dessem D, Taylor A (1989) Morphology of jaw-muscle spindle afferents in the rat. J Comp Neurol 282:389–403. https://doi.org/10.1002/cne.902820306

Dimova RN, Markov DV (1976) Changes in the mitochondria in the initial part of the axon during regeneration. Acta Neuropath 36:235–242

Espana A, Clotman F (2012) Onecut factors control development of the locus coeruleus and of the mesencephalic trigeminal nucleus. Mol Cell Neurosci 50:93–102. https://doi.org/10.1016/j.mcn.2012.04.002

Giovanni A, Giorgia A (2021) The neurophysiological basis of bruxism. Heliyon 7:e07477. https://doi.org/10.1016/j.heliyon.2021.e07477

Hassanali J (1997) Quantitative and somatotopic mapping of neurons in the trigeminal mesencephalic nucleus and ganglion innervating teeth in monkey and baboon. Arch Oral Biol 42:673–682. https://doi.org/10.1016/s0003-9969(97)00081-2

Hinrichsen CF (1970) Coupling between cells of the trigeminal mesencephalic nucleus. J Dent Res 49(Suppl):1369–1373. https://doi.org/10.1177/00220345700490063701

Honma S, Moritani M, Zhang LF, Lu LQ, Yoshida A, Appenteng K, Shigenaga Y (2001) Quantitative ultrastructure of synapses on functionally identified primary afferent neurons in the cat trigeminal mesencephalic nucleus. Exp Brain Res 137:150–162. https://doi.org/10.1007/s002210000632

Iida C, Oka A, Moritani M et al (2010) Corticofugal direct projections to primary afferent neurons in the trigeminal mesencephalic nucleus of rats. Neuroscience 169:1739–1757. https://doi.org/10.1016/j.neuroscience.2010.06.031

Ishii T, Furuoka H, Itou T, Kitamura N, Nishimura M (2005) The mesencephalic trigeminal sensory nucleus is involved in the control of feeding and exploratory behavior in mice. Brain Res 1048:80–86. https://doi.org/10.1016/j.brainres.2005.04.038

Ishii T, Furuoka H, Kitamura N, Muroi Y, Nishimura M (2006) The mesencephalic trigeminal sensory nucleus is involved in acquisition of active exploratory behavior induced by changing from a diet of exclusively milk formula to food pellets in mice. Brain Res 1111:153–161. https://doi.org/10.1016/j.brainres.2006.06.098

Kishimoto H, Bae YC, Yoshida A et al (1998) Central distribution of synaptic contacts of primary and secondary jaw muscle spindle afferents in the trigeminal motor nucleus of the cat. J Comp Neurol 391:50–63

Lazarov N (1995) Distribution of calcitonin gene-related peptide- and neuropeptide Y-like immunoreactivity in the trigeminal ganglion and mesencephalic trigeminal nucleus of the cat. Acta Histochem 97:213–223. https://doi.org/10.1016/S0065-1281(11)80102-9

Lazarov N (1996) Fine structure and synaptic organization of the mesencephalic trigeminal nucleus of the cat: a quantitative electron microscopic study. Eur J Morphol 34:95–106. https://doi.org/10.1076/ejom.34.2.95.13018

Lazarov NE (2000) The mesencephalic trigeminal nucleus in the cat. Adv Anat Embryol Cell Biol 153:1–103. https://doi.org/10.1007/978-3-642-57176-3. (**iii–xiv**)

Lazarov NE, Chouchkov CN (1996) Peptidergicinnervationofthemesencephalictrigeminalnucleusinthecat. Anat Rec 245:581–592. https://doi.org/10.1002/(SICI)1097-0185(199607)245:3%3c581::AID-AR15%3e3.0.CO;2-L

Lazarov N, Pilgrim C (1997) Localization of D1 and D2 dopamine receptors in the rat mesencephalic trigeminal nucleus by immunocytochemistry and in situ hybridization. Neurosci Lett 236:83–86. https://doi.org/10.1016/s0304-3940(97)00761-1

Lazarov NE, Usunoff KG, Schmitt O, Itzev DE, Rolfs A, Wree A (2011) Amygdalotrigeminal projection in the rat: an anterograde tracing study. Ann Anat 193:118–126. https://doi.org/10.1016/j.aanat.2010.12.004

Liem RS, Copray JC, van Willigen JD (1991) Ultrastructure of the rat mesencephalic trigeminal nucleus. Acta Anat (basel) 140:112–119. https://doi.org/10.1159/000147045

Liem RS, Copray JC, van Willigen JD (1992) Distribution of synaptic boutons in the mesencephalic trigeminal nucleus of the rat—a quantitative electron-microscopical study. Acta Anat (basel) 143:74–78. https://doi.org/10.1159/000147231

Liem RS, Copray JC, Van der Want JJ (1997) Dopamine-immunoreactivity in the rat mesencephalic trigeminal nucleus: an ultrastructural analysis. Brain Res 755:319–325. https://doi.org/10.1016/s0006-8993(97)00124-8

Liu X, Zhang C, Wang D, Zhang H, Liu X, Li J, Wang M (2017) Proprioceptive mechanisms in occlusion-stimulated masseter hypercontraction. Eur J Oral Sci 125:127–134. https://doi.org/10.1111/eos.12331

Liu X, Zhou KX, Yin NN et al (2019) Malocclusion generates anxiety-like behavior through a putative lateral habenula-mesencephalic trigeminal nucleus pathway. Front Mol Neurosci 12:174. https://doi.org/10.3389/fnmol.2019.00174

Luo P, Dessem D (1996) Morphological evidence for recurrent jaw-muscle spindle afferent feedback within the mesencephalic trigeminal nucleus. Brain Res 710:260–264. https://doi.org/10.1016/0006-8993(95)01439-x

Luo PF, Li JS (1991) Monosynaptic connections between neurons of trigeminal mesencephalic nucleus and jaw-closing motoneurons in the rat: an intracellular horseradish peroxidase labelling study. Brain Res 559:267–275

Luo PF, Wang BR, Peng ZZ, Li JS (1991) Morphological characteristics and terminating patterns of masseteric neurons of the mesencephalic trigeminal nucleus in the rat: an intracellular horseradish peroxidase labeling study. J Comp Neurol 303:286–299. https://doi.org/10.1002/cne.903030210

Mascaro MB, Prosdocimi FC, Bittencourt JC, Elias CF (2009) Forebrain projections to brainstem nuclei involved in the control of mandibular movements in rats. Eur J Oral Sci 117:676–684. https://doi.org/10.1111/j.1600-0722.2009.00686.x

Minkels RF, Juch PJ, Ter Horst GJ, Van Willigen JD (1991) Projections of the parvocellular reticular formation to the contralateral mesencephalic trigeminal nucleus in the rat. Brain Res 547:13–21. https://doi.org/10.1016/0006-8993(91)90569-h

Nomura S, Mizuno N (1985) Differential distribution of cell bodies and central axons of mesencephalic trigeminal nucleus neurons supplying the jaw-closing muscles and periodontal tissue: a transganglionic tracer study in the cat. Brain Res 359:311–319. https://doi.org/10.1016/0006-8993(85)91442-8

Nomura S, Konishi A, Itoh K, Sugimoto T, Yasui Y, Mitani A, Mizuno N (1985) Multipolar neurons and axodendritic synapses in the mesencephalic trigeminal nucleus of the cat. Neurosci Lett 55:337–342. https://doi.org/10.1016/0304-3940(85)90458-6

Ohara H, Tachibana Y, Fujio T et al (2016) Direct projection from the lateral habenula to the trigeminal mesencephalic nucleus in rats. Brain Res 1630:183–197. https://doi.org/10.1016/j.brainres.2015.11.012

Ohno N, Kidd GJ, Mahad D, Kiryu-Seo S, Avishai A, Komuro H, Trapp BD (2011) Myelination and axonal electrical activity modulate the distribution and motility of mitochondria at CNS nodes of Ranvier. J Neurosci 31:7249–7258. https://doi.org/10.1523/JNEUROSCI.0095-11.2011

Olucha F, Martinez-Garcia F, Lopez-Garcia C (1985) A new stabilizing agent for the tetramethyl benzidine (TMB) reaction product in the histochemical detection of horseradish peroxidase (HRP). J Neurosci Methods 13:131–138. https://doi.org/10.1016/0165-0270(85)90025-1

Paik SK, Kwak MK, Ahn DK et al (2005) Ultrastructure of jaw muscle spindle afferents within the rat trigeminal mesencephalic nucleus. NeuroReport 16:1561–1564. https://doi.org/10.1097/01.wnr.0000180149.29762.c4

Perkins E, Warren S, May PJ (2009) The mesencephalic reticular formation as a conduit for primate collicular gaze control: tectal inputs to neurons targeting the spinal cord and medulla. Anat Rec (hoboken) 292:1162–1181. https://doi.org/10.1002/ar.20935

Sato K (2021) Why is the mesencephalic nucleus of the trigeminal nerve situated inside the brain? Med Hypotheses 153:110626. https://doi.org/10.1016/j.mehy.2021.110626

Shigenaga Y, Mitsuhiro Y, Yoshida A, Cao CQ, Tsuru H (1988a) Morphology of single mesencephalic trigeminal neurons innervating masseter muscle of the cat. Brain Res 445:392–399. https://doi.org/10.1016/0006-8993(88)91206-1

Shigenaga Y, Yoshida A, Mitsuhiro Y, Doe K, Suemune S (1988b) Morphology of single mesencephalic trigeminal neurons innervating periodontal ligament of the cat. Brain Res 448:331–338. https://doi.org/10.1016/0006-8993(88)91272-3

Shigenaga Y, Doe K, Suemune S et al (1989) Physiological and morphological characteristics of periodontal mesencephalic trigeminal neurons in the cat–intra-axonal staining with HRP. Brain Res 505:91–110. https://doi.org/10.1016/0006-8993(89)90119-4

Shirasu M, Takahashi T, Yamamoto T, Itoh K, Sato S, Nakamura H (2011) Direct projections from the central amygdaloid nucleus to the mesencephalic trigeminal nucleus in rats. Brain Res 1400:19–30. https://doi.org/10.1016/j.brainres.2011.05.026

Takahashi T, Shirasu M, Shirasu M et al (2010) The locus coeruleus projects to the mesencephalic trigeminal nucleus in rats. Neurosci Res 68:103–106. https://doi.org/10.1016/j.neures.2010.06.012

Wang N, May PJ (2008) Peripheral muscle targets and central projections of the mesencephalic trigeminal nucleus in macaque monkeys. Anat Rec (hoboken) 291:974–987. https://doi.org/10.1002/ar.20712

Yabuta NH, Yasuda K, Nagase Y, Yoshida A, Fukunishi Y, Shigenaga Y (1996) Light microscopic observations of the contacts made between two spindle afferent types and alpha-motoneurons in the cat trigeminal motor nucleus. J Comp Neurol 374:436–450. https://doi.org/10.1002/(SICI)1096-9861(19961021)374:3%3c436::AID-CNE8%3e3.0.CO;2-2

Yokomizo Y, Murai Y, Tanaka E, Inokuchi H, Kusukawa J, Higashi H (2005) Excitatory GABAergic synaptic potentials in the mesencephalic trigeminal nucleus of adult rat in vitro. Neurosci Res 51:463–474. https://doi.org/10.1016/j.neures.2004.12.016

Yoshida S, Oka H (1998) Membrane properties of dissociated trigeminal mesencephalic neurons of the adult rat. Neurosci Res 30:227–234. https://doi.org/10.1016/s0168-0102(98)00003-0

Yoshida A, Moritani M, Nagase Y, Bae YC (2017) Projection and synaptic connectivity of trigeminal mesencephalic nucleus neurons controlling jaw reflexes. J Oral Sci 59:177–182. https://doi.org/10.2334/josnusd.16-0845

Zhao YJ, Liu Y, Wang J et al (2022) Activation of the mesencephalic trigeminal nucleus contributes to masseter hyperactivity induced by chronic restraint stress. Front Cell Neurosci 16:841133. https://doi.org/10.3389/fncel.2022.841133